Acta Crystallographica Section C
Crystal Structure Communications
ISSN 0108-2701

Monoclinic PZN-8%PT [$Pb(Zn_{0.3066}Nb_{0.6133}Ti_{0.08})O_3$] at 4 K

Jennifer S. Forrester* and Erich H. Kisi

School of Engineering, University of Newcastle, New South Wales 2308, Australia
Correspondence e-mail: jenny.forrester@newcastle.edu.au

Received 5 September 2007
Accepted 15 October 2007
Online 30 November 2007

The structure of the relaxor ferroelectric $Pb(Zn_{0.3066}Nb_{0.6133}Ti_{0.08})O_3$ (lead zinc niobium titanium trioxide), known as PZN-8%PT, was determined at 4 K from very high resolution neutron powder diffraction data. The material is known for its extraordinary piezoelectric properties, which are closely linked to the structure. Pseudo-cubic lattice parameters have led to considerable controversy over the symmetry of the structure. We find the structure to be monoclinic in the space group *Cm* (No. 8), with the Zn, Nb and Ti cations sharing the octahedrally coordinated *B* site (site symmetry *m*, special position 2*a*) and Pb occupying the 12-coordinate *A* site (site symmetry *m*, special position 2*a*). O atoms occupy a disorted octahedron around the *B* site (site symmetry *m* and special position 2*a*, and site symmetry 1 and general position 4*b*). Atomic coordinates have been determined for the first time, allowing the direction of spontaneous polarization to be visualized.

Comment

The crystal structure of the perovskite relaxor ferroelectric $Pb(Zn_{1/3}Nb_{2/3})O_3$ (lead zinc niobate or PZN) and its alloys with $PbTiO_3$ (PZN-PT) is of interest due to the outstanding piezoelectric properties of these compounds (*e.g.* Park & Shrout, 1997). PZN-PT is a solid solution with multiple occupancy of the perovskite *B* site by Zn, Nb and Ti. The crystal structure–property relationship in PZN-PT is poorly understood, due to extreme pseudosymmetry and the unavailability of single-domain single crystals. One feature that is certain and which adds to the mystique is that the maximum piezoelectric response is along [001] of the parent cubic phase, whereas the spontaneous polarization is along [111] of the ferroelectrically distorted crystals over a wide composition range. The region where the highest piezoelectric properties have been measured is at the morphotropic phase boundary (MPB) PZN-8%PT. This is the composition range where the rhombohedral PZN structure (*R*3*m*) meets the tetragonal $PbTiO_3$ structure (*P*4*mm*).

The structure of PZN-8%PT and of MPB phases in general has been widely debated. The systems $PbZrO_3$–$PbTiO_3$ (PZT) and $Pb(Mn_{1/3}Nb_{2/3})O_3$–$PbTiO_3$ (PMN-PT) are considered analogue systems. Previous work on PZN-PT has relied on synchrotron X-ray (Noheda *et al.*, 2001; Cox *et al.*, 2001) and neutron diffraction (Ohwada *et al.*, 2001) reciprocal space scans around a limited number of reflections from poly-domain single crystals and X-ray powder diffraction (Ohwada *et al.*, 2001; Noheda *et al.*, 2002; La-Orauttapong *et al.*, 2002). These experimental studies have focused on the lattice symmetry. The pseudo-cubic nature of the structure has made the determination of the true symmetry extremely difficult, even with three-axis diffractometers (Noheda *et al.*, 2002).

Many papers have implicated structural phase transitions in the piezoelectric response of these materials. Originally, an electric-field induced phase transition from rhombohedral (*R*3*m*) to tetragonal (*P*4*mm*) was proposed (Park & Shrout, 1997; Paik *et al.*, 1999; Durbin *et al.*, 1999). In recent years, many variations have been proposed in the region of the MPB in both PZN-PT and PZT. A monoclinic phase (*Cm*) rather than the traditional *R*3*m*+*P*4*mm* co-existence at the MPB in PZT was first observed by Noheda *et al.* (1999) and a new phase diagram was proposed which incorporates this phase (Noheda *et al.*, 2000). This monoclinic phase was explained as a bridging structure between *R*3*m* and *P*4*mm*, as there is no symmetry axis, just a mirror plane. This mirror plane is the only symmetry element common to *R*3*m* and *P*4*mm*. The MPB in both PZN-PT and PZT has since been studied by many groups. One suggestion is that this region is in fact orthorhombic in the space group *Amm*2 (La-Orauttapong *et al.*, 2002). Many other phases or combinations of phases have been proposed at the MPBs. These include but are not restricted to *R*3*c*+*Cm* (Frantti *et al.*, 2003), *Pm* (Bertram *et al.*, 2003), *Cm*+*Cc* (Ranjan *et al.*, 2005) and *Cc* (Woodward *et al.*, 2005). These studies have included analogue systems PZT and PMN-PT, studies of poled PZN-PT crystals (*e.g.* Marssi & Dammak, 2007) and studies of PZN-PT with applied electric fields (*e.g.* Viehland *et al.*, 2001). Results for PZN-PT materials have been postulated from a consideration of lattice symmetry only; no ion coordinates have been published other than for PZN (Kisi *et al.*, 2006). Given that the spontaneous and induced polarizations depend on ion coordinates and not lattice symmetry, there is an urgent need for the ground state of PZN-8%PT to be known.

Structural variations between the possible structures are largely due to differences in the O-ion coordinates, giving a strong motivation for the use of neutron diffraction. The presence of ferroelectric domains makes the refinement of ion coordinates from standard single-crystal data very difficult. Consequently, this paper presents the crystal structure determination and refinement for $Pb(Zn_{0.3066}Nb_{0.6133}Ti_{0.08})O_3$ (PZN-8%PT) using very high resolution neutron powder diffraction. We find that the ground state of PZN-8%PT is monoclinic in the space group *Cm*. The principal direction of the spontaneous polarization is close to $[100]_M = [110]_C$.

 doi:10.1107/S0108270107050640

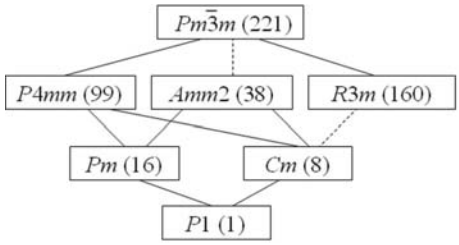

Figure 1
Group–subgroup relationships among the ferroelectric perovskite space groups. Space groups connected by solid lines are allowed to undergo continuous phase transitions under Landau theory, whereas those joined by dashed lines are not. (Reproduced from Forrester *et al.* (2001) with the permission of IOP Publishing Ltd.)

Experimental

Single crystals of PZN-8%PT were grown in a PbO flux using a ratio of 35% PZN-8%PT to 65% flux. Powders were placed in a platinum crucible and held at 1473 K for 2 h. The sample was cooled at a rate of approximately 1 K h^{-1} to 1173 K and then at a rate of 50 K h^{-1} to room temperature. Crystals were extracted using a hot HNO_3 solution, lightly crushed and passed through a 143 µm sieve. Approximately 2 ml of the coarse powder was loaded into a thin-walled aluminium can for data collection on the HRPD diffractometer (resolution $\Delta d/d \simeq 4 \times 10^{-4}$) at the ISIS facility, Rutherford Appleton Laboratory, Didcot, UK. The sample was cooled in a liquid helium cryostat to 4 K. After equilibrating at this temperature, diffraction data were recorded from 30 to 120 ms for 90 min.

Crystal data

$Pb(Zn_{0.3066}Nb_{0.6133}Ti_{0.08})O_3$
M_r = 336.06
Monoclinic, *Cm*
a = 5.7461 (2) Å
b = 5.7278 (2) Å
c = 4.0409 (3) Å
β = 90.155 (3)°
V = 133.00 (1) Å^3
Z = 2
Neutron radiation
λ = 0.65–2.45 Å
T = 4 K
Specimen shape: powder
Specimen prepared at 0 kPa
Specimen prepared at 1473 K
Particle morphology: powder, pale yellow

Data collection

Powder diffractometer
Specimen mounting: 11mm Al slab can
Specimen mounted in transmission mode
Scan method: time of flight

Refinement

R_p = 0.091
R_{wp} = 0.111
R_{exp} = 0.087
S = 1.28
Wavelength of incident radiation: 0.65–2.45 Å
Excluded region(s): none
Profile function: TOF profile function number 4 with 21 terms
Number of reflections: 254
34 parameters
$(\Delta/\sigma)_{max}$ = 0.43
Preferred orientation correction: none

Rietveld analyses used the program *GSAS* (Larson & Von Dreele, 1994). Only the data from the high-resolution backscattering bank were used in the refinement. Typically, lattice parameters, atom coordinates (Zn/Nb/Ti, O), isotropic displacement parameters, scale, four polynomial background parameters and two isotropic peak profile parameters were refined. The anisotropic peak-broadening model of Stephens (1999) was necessary to obtain acceptable fits in any space group.

As the crystal structures in the PZN-PT system are pseudo-cubic, it is not possible to use single-peak or even peak deconvolution techniques to assess their symmetry. Instead, the structure of PZN-8%PT was assessed through a long series of Rietveld refinements. A group theoretical analysis by Forrester *et al.* (2001) has given the potential space groups and their relationships in the absence of octahedral tilting, as reproduced in Fig. 1. Space groups resulting from coupling of octahedral tilting with the ferroelectric distortion have been determined by Stokes *et al.* (2002), but were not considered here as no superlattice peaks due to octahedral tilting were detected. Within Fig. 1, only *P*1 has not been proposed as the space group of the MPB phase(s) in PZN-PT. The refinements were therefore conducted in all the space groups in the diagram except *P*1 and the parent cubic structure, *Pm*3*m*. Each of the refinements was given equal opportunity to fit, refining the same set of parameters in as many sensible ways as possible from numerous starting positions. The refined lattice parameters, atomic coordinates and isotropic displacement parameters are available in the supplementary materials.

In examining the output of the Rietveld refinements, the usual statistical measures were found to be not sensitive enough to discriminate between some closely competing models. Instead, certain diagnostic peaks (reflections) were found to discriminate well between the models when consulted in sufficient detail. In particular, the 200 peak is so oddly shaped that it was found that particular attention to the peak-shape parameters was required in order to obtain a fit to that part of the pattern. This and the other diagnostic peaks from each of the refinements are shown in Fig. 2. It is probably no accident that the most useful diagnostic peaks (200, 220 and 222) occur when the scattering vector is perpendicular to the three principal directions in the Devonshire expansion of the free energy of a ferroelectric (Devonshire, 1949, 1951). The refinement results are now discussed in turn, beginning with the simplest and ending with the most probable solution.

*R*3*m* (Fig. 2*a*): The phase diagram of Kuwata *et al.* (1981) suggests that the rhombohedral ferroelectric phase extends beyond 8%PT at cryogenic temperatures. Combined with our observations of a rhombohedral ground state in PZN and PZN-4.5%PT (Kisi *et al.*, 2005; Forrester *et al.*, 2006), this was the logical starting point. Although superficially the fit of the overall pattern to *R*3*m* looks good (*e.g.* on the same scale as Fig. 3), there are areas of significant misfit that could not be corrected. This is most easily observable in the 200 and 222 peaks, but is present in all of the diffraction peaks to some degree. The 200 peak in Fig. 2(*a*) clearly has a second peak on the low-*d* side, and therefore a two-phase refinement was the logical progression.

*R*3*m*+*P*4*mm*, *c* > *a* (Fig. 2*b*): In the older literature, this two-phase mixture was the accepted state of samples in the MPB region of PZT ceramics. It is also a logical structure in PZN-8%PT (*i.e.* at the MPB) between the *R* region at <8%PT and the *T* region at >9%PT, according to older literature (*e.g.* Kuwata *et al.*, 1981). The Rietveld refinement is again superficially reasonable on the scale of Fig. 3 (73% *R*3*m* + 27% *P*4*mm*). The lattice parameters and peak-width parameters can be manipulated to make the 200 peak fit very well. However, the lattice parameters of the *R* and *T* phases cannot be fitted to both the *h*00 and *hhh* peaks concurrently. If the 200 peak is forced to fit, then *hhh* moves outside the low-*d* side of the experimental peak envelope. The fit shown in Fig. 2(*b*) is the 'average' fit obtained by free refinement of the lattice parameters. The fit is worse than for the single-phase rhombohedral model. The only way to model the 200 peak correctly and force the calculated 222 position to lie within the observed {222} envelope was to set the *a* and *c* lattice

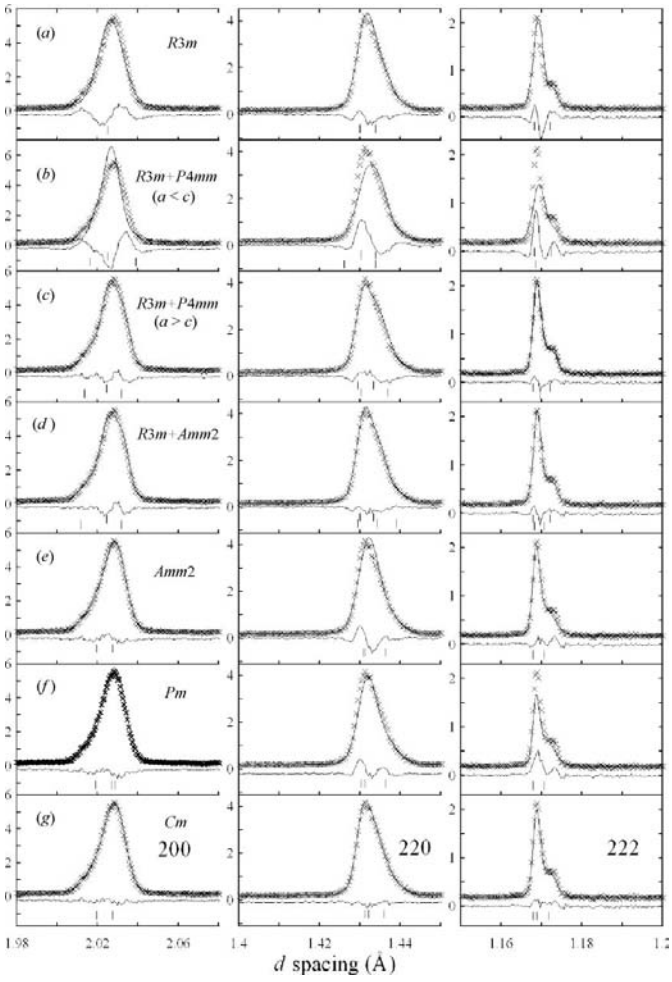

Figure 2
Diagnostic peaks within the Rietveld fits, showing the 200, 220 and 222 diffraction peaks illustrating the structures tested. (*a*) *R*3*m*, (*b*) *R*3*m* and *P*4*mm* ($a < c$), (*c*) *R*3*m* and *P*4*mm* ($a > c$), (*d*) *R*3*m* and *Amm*2, (*e*) *Amm*2, (*f*) *Pm* and (*g*) *Cm*.

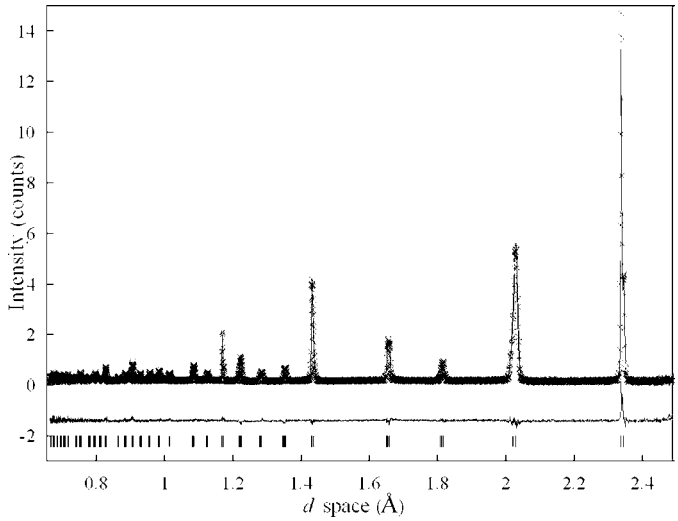

Figure 3
Rietveld refinement of PZN-8%PT at 4 K in the monoclinic space group *Cm*. The recorded data are shown as crosses (×), the calculated data as a continuous line, and the difference pattern and *hkl* markers are shown below.

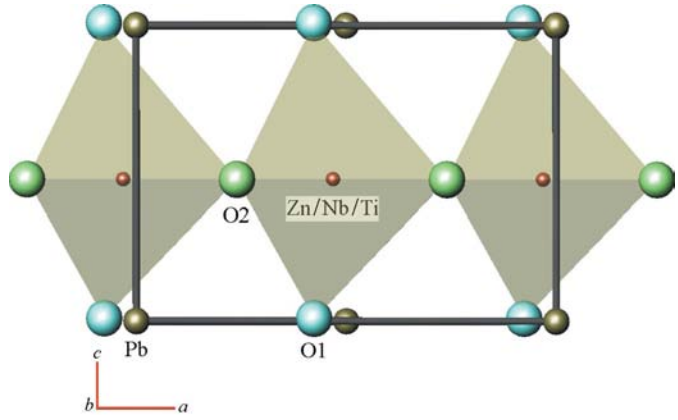

Figure 4
A projection of the monoclinic unit cell along *b*. The major ferroelectric distortion is seen to be along the *a* axis, with only minor distortion along the *c* axis.

parameters of the *T* phase such that $c < a$, which became the next model.

*R*3*m*+*P*4*mm*, $c < a$ (Fig. 2*c*): Although a tetragonal ferroelectric with $a > c$ is a physically unreasonable structure, as an exercise in data analysis this refinement converged to a much improved fit compared with the previous two. The refined phase proportions are 72% *R*3*m* + 28% *P*4*mm*. Although the fit has greatly improved, there are slight misfits in the very top of the 200 peak and at the high-*d* side of the 220 peak, which could not be corrected with additional parameters or damped refinements. Analysis of the possible phases (Fig. 1) indicates that a pseudo-tetragonal phase with $c < a$ would be orthorhombic in the space group *Amm*2.

*R*3*m*+*Amm*2 (Fig. 2*d*): The fit to the 200 and 222 peaks here is nearly identical to the previous fit, as are the refined phase proportions (84% *R*3*m* + 16% *Amm*2) if corrected for cell doubling in the orthorhombic structure. The 220 peak is improved by the additional degrees of freedom given in the orthorhombic space group. Nonetheless, the misfits at the 200 and 222 peaks remain. Although they may seem minor, in this system where little separates the correct from the incorrect this solution must be rejected.

When fully orthorhombic or monoclinic solutions were initially attempted, satisfactory fits could not be obtained. In general, agreement was worse than for *R*3*m*+*P*4*mm* with $a < c$ (Fig. 2*b*). Later trials revealed that this was due to a too-conservative application of the anisotropic broadening correction (Stephens, 1999), comprising just two or three of the available anisotropic broadening parameters (six for orthorhombic and nine for monoclinic). Once the full broadening parameter set was released, coupled with the structural parameters, quite reasonable and potentially convincing fits were obtained in the three space groups, *Amm*2, *Pm* and *Cm*, associated with the polarization rotation theory and prior synchrotron studies (Noheda *et al.*, 2001; Vanderbilt & Cohen, 2001).

*Amm*2 (Fig. 2*e*): The fit in *Amm*2 is of the same overall quality as the fit in the *R*3*m*+*Amm*2 model but with many fewer parameters. Improved agreement is observed for the 200 and 222 peaks. However, the 220 peak does not fit well.

Pm (Fig. 2*f*): The refinements here produced inferior agreement with the data, which is easily visible in the 220 and 222 peaks.

Cm (Fig. 2*g*): The figure clearly shows that the space group *Cm* produces a superior fit compared with any of the other options. For completeness, two-phase refinements were attempted using *Cm*+*R*3*m*

and *Cm*+*P*4*mm*, with no further improvement over the single-phase *Cm* refinement shown in Fig. 2(*g*).

From the above, it was concluded that the space group of PZN-8%PT at 4 K is *Cm*. The Rietveld refinement using that space group is shown in full in Fig. 3 and the structure is illustrated in Fig. 4.

Data collection: ISIS in-house software; cell refinement: *GSAS* (Larson & Von Dreele, 1994); data reduction: ISIS in-house software; program(s) used to solve structure: *GSAS*; program(s) used to refine structure: *GSAS*; molecular graphics: *ATOMS* (Dowty, 2005); software used to prepare material for publication: *enCIFer* (Allen *et al.*, 2004).

The authors express many thanks to Dr Kevin Knight of ISIS for assistance with the data collection. This work has been supported by the Australian Research Council (grant No. DP-0666166) and the Access to Major Research Facilities Programme.

Supplementary data for this paper are available from the IUCr electronic archives (Reference: SQ3101). Services for accessing these data are described at the back of the journal.

References

Allen, F. H., Johnson, O., Shields, G. P., Smith, B. R. & Towler, M. (2004). *J. Appl. Cryst.* **37**, 335–338.
Bertram, R., Reck, G. & Uecker, R. (2003). *J. Cryst. Growth*, **253**, 212–220.
Cox, D. E., Noheda, B., Shirane, G., Uesu, Y., Fujishiro, K. & Yamada, Y. (2001). *Appl. Phys. Lett.* **79**, 400–402.
Devonshire, A. F. (1949). *Philos. Mag.* **40**, 1040–1063.
Devonshire, A. F. (1951). *Philos. Mag.* **42**, 1065–1079.
Dowty, E. (2005). *ATOMS*. Version 6.2. Shape Software, Kingsport, Tennessee, USA.
Durbin, M. K., Jacobs, E. W., Hicks, J. C. & Park, S.-E. (1999). *Appl. Phys. Lett.* **74**, 2848–2850.
Forrester, J. S., Kisi, E. H. & Knight, K. S. (2006). *Physica B*, **385–386**, 160–162.
Forrester, J. S., Piltz, R. O., Kisi, E. H. & McIntyre, G. J. (2001). *J. Phys. Condens. Matter*, **13**, L825–L833.
Frantti, J., Eriksson, S., Hull, S., Lantto, V., Rundlof, H. & Kakihana, M. (2003). *J. Phys. Condens. Matter*, **15**, 6031–6041.
Kisi, E. H., Forrester, J. S. & Knight, K. S. (2005). *J. Phys. Condens. Matter*, **17**, L381–L384.
Kisi, E. H., Forrester, J. S. & Knight, K. S. (2006). *Acta Cryst.* C**62**, i46–i48.
Kuwata, J., Uchino, K. & Nomura, S. (1981). *Ferroelectrics*, **37**, 579–582.
La-Orauttapong, D., Noheda, B., Ye, Z.-G., Gehring, P. M., Toulouse, J., Cox, D. E. & Shirane, G. (2002). *Phys. Rev. B*, **65**, 144101.
Larson, A. C. & Von Dreele, R. B. (1994). *GSAS*. Report LAUR 86-748. Los Alamos National Laboratory, New Mexico, USA.
Marssi, M. L. & Dammak, H. (2007). *Solid State Commun.* **142**, 487–491.
Noheda, B., Cox, D. E., Shirane, G., Gonzalo, J. A., Cross, L. E. & Park, S.-E. (1999). *Appl. Phys. Lett.* **74**, 2059–2061.
Noheda, B., Cox, D. E., Shirane, G., Park, S.-E., Cross, L. E. & Zhong, Z. (2001). *Phys. Rev. Lett.* **86**, 3891–3894.
Noheda, B., Gonzalo, J. A., Cross, L. E., Guo, R., Park, S.-E., Cox, D. E. & Shirane, G. (2000). *Phys. Rev. B*, **61**, 8687–8695.
Noheda, B., Zhong, Z., Cox, D. E., Shirane, G., Park, S.-E. & Rehring, P. (2002). *Phys. Rev. B*, **65**, 224101.
Ohwada, K., Hirota, K., Rehrig, P. W., Gehring, P. M., Noheda, B., Fujii, Y., Park, S.-E. E. & Shirane, G. (2001). *J. Phys. Soc. Jpn*, **70**, 2778–2783.
Paik, D.-S., Park, S.-E., Wada, S., Liu, S.-F. & Shrout, T. R. (1999). *J. Appl. Phys.* **85**, 1080–1083.
Park, S.-E. & Shrout, T. R. (1997). *J. Appl. Phys.* **82**, 1804–1811.
Ranjan, R., Singh, A. K., Ragini & Pandey, G. (2005). *Phys. Rev. B*, **71**, 092101.
Stephens, P. W. (1999). *J. Appl. Cryst.* **32**, 281–289.
Stokes, H. T., Kisi, E. H., Hatch, D. M. & Howard, C. J. (2002). *Acta Cryst.* B**58**, 934–938.
Vanderbilt, D. & Cohen, M. H. (2001). *Phys. Rev. B*, **63**, 094108.
Viehland, D., Amin, A. & Li, J. F. (2001). *Appl. Phys. Lett.* **79**, 1006–1008.
Woodward, D. I., Knudsen, J. & Reaney, I. M. (2005). *Phys. Rev. B*, **72**, 104110.